Acta Crystallographica Section B
Structural Science
ISSN 0108-7681

Structure and phase transitions of $LiTaOGeO_4$

Thomas Malcherek

Institut für Mineralogie, Westfälische Wilhelms Universität Münster, Corrensstrasse 24, D-48149 Münster, Germany

Correspondence e-mail: malcher@nwz.uni-muenster.de

Received 22 August 2001
Accepted 7 May 2002

The structure of $LiTaOGeO_4$ has been refined using X-ray diffraction data collected at 293 K and at 173 K. The low-temperature structure is isostructural with $LiTaOSiO_4$ and closely related to the low-temperature structure of titanite, $CaTiOSiO_4$. Li occurs in a distorted tetrahedral coordination. The transition to the disordered structure, with space group symmetry $C2/c$, occurs at $T_c = 231\ (1)$ K. Li is disordered across two symmetry-equivalent positions and Ta is located at the centre of its coordination octahedron in this paraphase. The transition is continuous, and the thermal evolution of the order parameter is well approximated using a tricritical mean-field model. Anharmonic thermal displacement of the Li cation has been analyzed and its one-particle potential has been determined. The height of the potential barrier separating the two Li positions across a curved trajectory is close to RT_c, where R is the universal gas constant.

1. Introduction

A large number of compounds of general composition $AMOXO_4$ crystallize with the topology of the titanite structure. This structure type is formed by parallel chains of corner-sharing *trans*-connected MO_6 octahedra, coupled *via* individual XO_4 tetrahedra. Each tetrahedron links two consecutive octahedra of one chain to octahedra in two neighbouring chains. Cavities in the resulting $[MOXO_4]$ framework may be occupied by cations A if such cations are required for charge balance.

One of these compounds, $LiTaOGeO_4$ (LTGO), was first described by Mill *et al.* (1990). The TaO_6 octahedra form nearly eclipsed *trans–trans* chains in LTGO and in $LiTaOSiO_4$ (LTSO) (Genkina & Mill, 1992), similar to the octahedral chains in β-$LiVOPO_4$ (Lii *et al.*, 1991). In titanite ($CaTiOSiO_4$), the octahedra are tilted in such a way that the equatorial O atoms do not overlap when projected parallel to the chain axis (Fig. 1).

In the high-temperature polymorph of titanite [space group (SG) symmetry $C2/c$], the Ti cation is nominally located at the centre of the TiO_6 octahedron, while the low-temperature form (SG symmetry $P2_1/c$) is characterized by the displacement of Ti towards the chain-forming corner O atom, O1 (Taylor & Brown, 1976). Such a displacement leads to the formation of alternating short and long $M-$O bonds in the chain direction. In the diffraction image it is accompanied by the appearance of superstructure maxima with indices $h + k = 2n + 1$. The square of the macroscopic off-centre Ti displacement correlates with the intensity of these maxima (Ghose *et al.*, 1991), which in turn relates it to the square of the order parameter of the transition. As the sense of the cation displacement is reversed among neighbouring octahedral

Table 1
Experimental details.

Crystal data			
Chemical formula	$GeLiO_5Ta$		
Chemical formula weight	340.48		
Radiation type	Mo $K\alpha$		
$F(000)$	592		
Z	4		
Crystal size (mm)	0.163 × 0.058 × 0.039		
Temperature (K)	173	293	
Crystal system, space group	Monoclinic, $P2_1/c$	Monoclinic, $C2/c$	
a, b, c (Å)	7.584 (4), 8.0849 (14), 7.508 (2)	7.5773 (1), 8.1188 (1), 7.4910 (1)	
β (°)	119.69 (3)	119.545 (1)	
V (Å^3)	399.9 (2)	400.91 (9)	
D_x (Mg m^{-3})	5.655	5.641	
No. of reflections for cell parameters	25	164	
μ (mm^{-1})	34.751	34.666	
Data collection			
Diffractometer	Enraf–Nonius CAD-4		
Data collection method	ω–2θ scans		
θ_{max} (°)	35		
Range of h, k, l	$-12 \rightarrow h \rightarrow 10$ $-13 \rightarrow k \rightarrow 13$ $0 \rightarrow l \rightarrow 12$		
No. of standard reflections	3		
No. of measured, independent and observed reflections	3561, 1732, 1476	1809, 877, 776	
Criterion for observed reflections	$I > 2\sigma(I)$	$I > 2\sigma(I)$	
R_{int}	0.032	0.023	
Absorption correction	Numerical	Numerical	
T_{min}	0.123	0.0705	
T_{max}	0.28	0.3450	
Refinement			
Refinement	Full-matrix least-squares on F^2		
Model	I	I	II
Weighting scheme	$w = 1/[\sigma^2(F_o^2) + (WP)^2]$ where $P = (F_o^2 + 2F_c^2)/3$		
W	0.0188	0.0217	0.0213
$R[F^2 > 2\sigma(F^2)]$, $wR(F^2)$, S	0.0207, 0.0465, 1.036	0.0159, 0.0374, 1.036	0.0158, 0.037, 1.036
No. of reflections, restraints and parameters used in refinement	1732, 0, 74	877, 0, 41	877, 0, 40
$(\Delta/\sigma)_{max}$	0.001	0.000	0.000
$\Delta\rho_{max}$, $\Delta\rho_{min}$ (e Å^{-3})	2.451, −2.697	1.943, −2.453	1.939, −2.43
Extinction coefficient	0.0318 (7)	0.0364 (10)	0.0367 (9)
Model	III	III	
Weighting scheme	$w = 1/[\sigma^2(F_o^2) + (WI_o)^2]$		
W	0.044	0.033	
$R[F^2 > 2\sigma(F^2)]$, $wR(F^2)$, S	0.0281, 0.0658, 1.005	0.0193, 0.0455, 1.015	
No. of reflections, restraints and parameters used in refinement	1496, 1, 98	784, 1, 53	
Extinction coefficient	0.397 (10) × 10^{-4}	0.433 (10) × 10^{-4}	

Computer programs used: *SHELXL*97 (Sheldrick, 1997), *PROMETHEUS* (Zucker *et al.*, 1983).

chains, the ordered polymorph of the titanite structure type constitutes an antiferroelectric.

A similarly ordered arrangement has been determined for the silicate LTSO (Genkina & Mill, 1992) under ambient conditions, while LTGO was found to be disordered (Mill *et al.*, 1990), with SG symmetry $C2/c$.

In titanite, the transition to the paraphase occurs in two steps (Kek *et al.*, 1997; Malcherek *et al.*, 2001). At $T_c = 487$ K, long-range correlation between the Ti displacements is lost in two dimensions, while linear correlation of the local displacements along the octahedral chain direction disappears only at $T_i = 825$ K (Zhang *et al.*, 1997).

As part of a larger investigation into phase transitions in compounds of the titanite structure type, the low-temperature structure of LTGO has been determined and its transition to the disordered structure has been followed, the results of which are reported here.

2. Experimental

Crystals of LTGO were grown from a GeO_2 flux following the method described by Mill *et al.* (1990). The obtained needle-shaped crystals were colourless and transparent, elongated parallel to [001] (in the $C2/c$ setting). Wavelength-dispersive electron-microprobe analysis confirmed a Ge/Ta ratio of 1.01 (0.01) in several crystals, and no impurities were observed in the electron-backscattering image. A suitable single crystal, bounded by the forms {001}, {110} and {$\bar{1}$10}, was selected for X-ray diffraction (XRD) measurements. The crystal quality was checked using precession photographs of the (20$\bar{4}$) × (100) reciprocal lattice plane. Intensity data were collected using an Enraf–Nonius CAD-4 diffractometer equipped with an N_2 gas stream cooling device. Room-temperature lattice constants were determined by Rietveld refinement of X-ray powder diffraction data using monochromatic Cu $K\alpha_1$ radiation. Crystal data and parameters of the data collections at 173 K and 293 K are listed in Table 1. The crystal was reoriented between the two measurements. The observed dimensions of the crystal were optimized using the program *X-SHAPE* (Stoe & Cie, 1996), based on the intensities of 49 unique reflections and their equivalents collected at 173 K. The resulting correction to the optically observed crystal dimensions improved R_{int} after correction for absorption considerably. Lorentz and polarization corrections and the numerical absorption correction were made using the program *X-RED* (Stoe & Cie, 1996). The structures were refined using *SHELXL*97 (Sheldrick, 1997) (models I and II, Table 1). The low-temperature structure refinement of $LiTaOGeO_4$ was started with the known structural parameters of $LiTaOSiO_4$. The starting parameters for the room-temperature structure were those of Mill *et al.* (1990).

Additional refinements were carried out using the *PROMETHEUS* program package (Zucker *et al.*, 1983) in order to determine anharmonic contributions to the temperature displacements of the Li atom (model III, Table 1). The anharmonic atomic displacements were described by third- and fourth-order cumulants in the Gram–Charlier expansion (Kuhs, 1992). An isotropic Becker & Coppens (1974) extinction correction of type 1 with a Lorentzian distribution of the mosaic spread (Zucker *et al.*, 1983) was applied. Only reflections with $I > 2\sigma(I)$ were used and the refinements were based on squared structure factors.

In addition, the intensities of the $10\bar{4}$ and $\bar{3}04$ superstructure reflections and of the adjacent fundamental reflections $11\bar{4}$, $1\bar{1}\bar{4}$, $\bar{3}14$ and $\bar{3}\bar{1}4$ were measured in the temperature range 161 K $\leq T \leq$ 287 K during heating and cooling. A set of 24 fundamental reflections was recentred at each measurement temperature and the orientation matrix was redetermined accordingly.

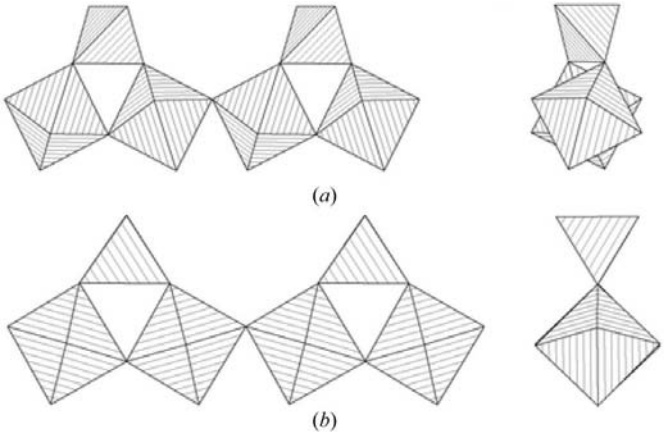

Figure 1
Octahedral chain conformation and orientation of the bridging XO_4 tetrahedra in titanite (*a*) and in the LTGO structure (*b*).

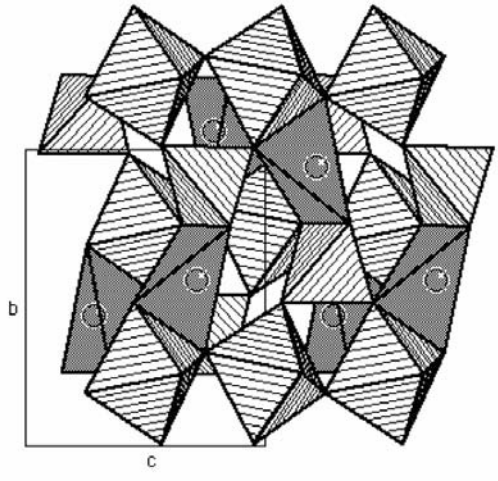

Figure 2
Polyhedral representation of the $LiTaOGeO_4$ structure along [100]. The Li atoms are shown inside their distorted tetrahedral coordination.

3. Results

The low-temperature structure determined at 173 K has SG symmetry $P2_1/c$. At this temperature, LTGO is isostructural to LTSO (Genkina & Mill, 1992) under ambient conditions. Ta is displaced by 0.07 Å towards the O1 atom. Unlike the Ti atom in the low-temperature phase of titanite, Ta is also displaced by about 0.04 Å towards the O32 atom. This particular O atom forms part of a GeO_4 tetrahedron that bridges two adjacent TaO_6 octahedra of one chain. In the LTGO structure this bridge runs nearly parallel to the chain direction, while in the titanite structure it does not because of the staggered arrangement of the octahedra (Fig. 1). Similar displacements have been determined for LTSO (Genkina & Mill, 1992), though the magnitude of the Ta displacement is larger in LTSO ($\simeq$ 0.09 Å $\parallel$ Ta—O1) in accordance with the higher T_c of LTSO, where the ordered structure is stable at room temperature.

As in $LiTaOSiO_4$, Li is four-coordinated in the low-temperature structure of LTGO. The distorted Li tetrahedra share two opposite edges with one TaO_6 octahedron and one GeO_4 tetrahedron, respectively (Fig. 2).

If the Li atom is located on the diad axis in the $C2/c$ high-temperature form, *i.e.* the special position 4*e* assumed by Mill *et al.* (1990) (model I), the resulting coordination of Li is fivefold and its displacement as a result of the phase transition would amount to almost 0.3 Å. However, based on the room-temperature XRD data reported here, the thermal displacement of Li appears very large and elongated parallel to [001] within this model (see supplementary material[1]). Instead, a model in which Li half occupies the 8*f* position yields an (isotropic) thermal displacement that is only slightly larger than the result at 173 K (model II). Owing to the small scattering power of Li, this approach does not significantly improve the refinement (Table 1). Nevertheless, the split-atom model appears more reasonable, based on the resulting similar thermal displacement at the two investigated temperatures. The local (or momentary) environment of the Li atom would therefore remain an elongated oxygen tetrahedron even in the high-temperature phase (Table 2). The displaced Li position nearly coincides with the position in the $P2_1/c$ phase, considering the origin shift of ($\frac{1}{4}$, $\frac{1}{4}$, 0) between the two phases (see supplementary material[1]).

In order to obtain this apparent Li disorder of the para-phase in a one-particle form, the anharmonic displacement of Li has been refined to the fourth order (model III). The resulting parameters are given in Table 3. R is reduced from 2.01% (R_w = 4.71%) in the harmonic model to 1.93% (R_w = 4.52%). The attempts to refine third- and fourth-order cumulants at first revealed strong correlation between γ_{222} and the free positional parameter y. While the mode positions, *i.e.* the position of the maxima of the resulting probability density function (PDF), were in good agreement with the results of model II, the height of the PDF and the value of y were heavily

[1] Supplementary data for this paper are available from the IUCr electronic archives (Reference: CK0010). Services for accessing these data are described at the back of the journal.

Table 2
Selected bond distances (Å) and angles (°).

173 K	Distance		Angle			
Model I						
Li		O1	O21	O22		
O1	1.976 (8)					
O21	2.004 (9)	136.4 (5)				
O22	2.024 (9)	135.6 (5)	81.2 (3)			
O31	2.082 (10)	81.6 (3)	110.0 (4)	110.5 (5)		
Ta		O1	O32	O21	O22	O31
O1	1.890 (3)					
O32	1.938 (3)	92.0 (1)				
O21	1.984 (3)	92.5 (1)	90.2 (1)			
O22	1.987 (3)	92.3 (1)	92.0 (1)	174.7 (1)		
O31	2.015 (3)	95.2 (1)	172.9 (1)	89.2 (1)	88.1 (1)	
O1′	2.025 (3)	177.2 (1)	90.8 (1)	88.1 (1)	87.1 (1)	82.1 (1)
Ge		O31	O32	O21		
O31	1.739 (3)					
O32	1.740 (3)	109.7 (2)				
O21	1.745 (3)	113.6 (1)	110.8 (1)			
O22	1.746 (3)	114.0 (1)	111.0 (1)	97.4 (1)		

293 K	Distance		Angle		
Model I					
Li		O1	O2′	O2	O3′
O1	1.994 (15)				
O2 (×2)	1.998 (11)	139.0 (3)	82.1 (5)		
O3 (×2)	2.400 (5)	75.1 (3)	101.5 (2)	100.9 (2)	150.2 (7)
Model II					
Li		O1	O2	O2′	O3
Li′	0.452 (29)				
O1	2.010 (14)				
O2	2.002 (16)	137.4 (9)			
O2′	2.014 (16)	136.6 (9)	81.6 (5)		
O3	2.183 (15)	79.9 (5)	108.5 (7)	108.9 (7)	
O3′	2.620 (14)	69.8 (4)	94.3 (6)	93.5 (6)	149.8 (6)
Ta		O1	O1′	O3	O3′
O1 (×2)	1.951 (1)				
O3 (×2)	1.974 (2)	93.2 (1)	86.8 (1)		
O2 (×2)	1.984 (2)	90.2 (1)	89.8 (1)	89.5 (1)	90.5 (1)
Ge		O3′	O3	O2′	
O3 (×2)	1.744 (2)	109.8 (2)			
O2 (×2)	1.742 (2)	112.3 (1)	112.1 (1)	97.8 (2)	

biased by a large positive value of γ_{222}. In the final refinement, y was therefore constrained to the value obtained in the harmonic approximation, which did not significantly affect the quality of the refinement or drastically alter the shape of the PDF. The constraint also ensured that for small displacements the PDF approaches the value of the harmonic contribution. The resulting PDF is plotted in Fig. 3(*a*). It shows that the two mode positions agree well with the results of the split-atom refinement. Using the Li PDF normalized by the height of these maxima, the corresponding one-particle potential (OPP) has been calculated (Fig. 4*a*) using the algorithms available in the *PROMETHEUS* package (pdfmap) (Zucker *et al.*, 1983). The probable movement of Li across the potential barrier is not parallel to [001] but curved along a pathway similar to the parabola drawn in Fig. 4(*a*). This particular pathway can be interpreted as the result of interactions with the three nearest O atoms. The time-averaged Li position marked by the tip of the parabola is about 0.1 Å closer to the O1 atom than the geometrical mean of the two mode positions. Thus the transition state between the two mode positions is characterized by a transient strengthening of the bond towards the O1 atom, while Li 'swings' about the edge of the GeO_4 tetrahedron formed by two O2 atoms (Fig. 5).

Fig. 4(*b*) traces the OPP along the curved trajectory of Fig. 4(*a*). The height of the potential barrier is 1960 J mol^{-1}. With a critical temperature of T_c = 231 K, this value is rather close to RT_c, where R is the universal gas constant. The

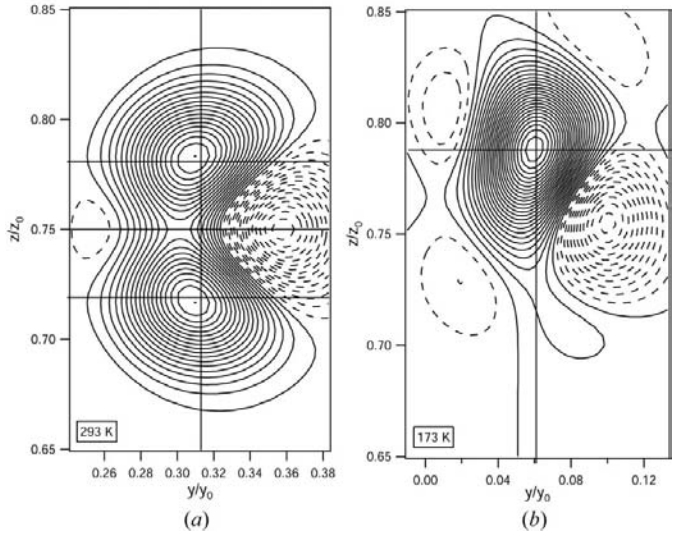

Figure 3
Li PDF parallel to (100) at (*a*) room temperature and (*b*) 173 K. The crossing lines mark the Li positions obtained in the harmonic model. The contour level spacings at 173 K are twice that at room temperature. Negative and thus undefined levels of the PDF are marked by dashed lines.

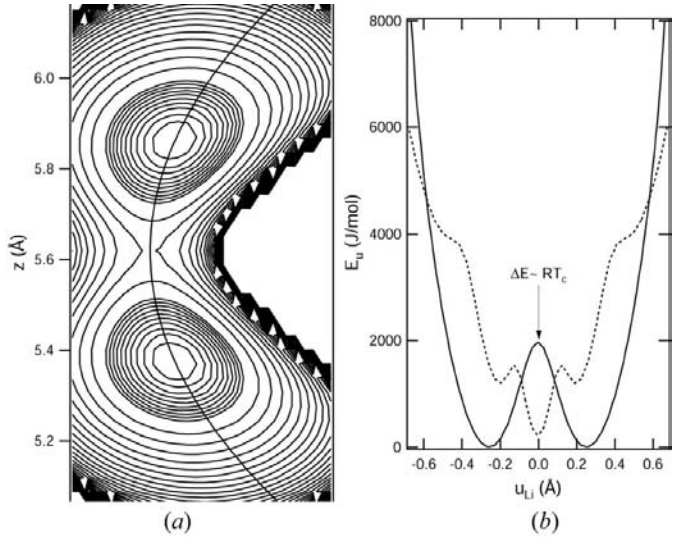

Figure 4
(*a*) One-particle potential as derived from the Li PDF of Fig. 3(*a*). The first ten contour levels are drawn at intervals of 100 J mol^{-1}; all following levels are 500 J mol^{-1} apart. (*b*) Trace of the potential along the curved trajectory shown in (*a*). The estimated error is marked by the dashed line. The height of the potential barrier is approximately RT_c.

Table 3
Third- and fourth-order tensorial coefficients γ_{ijk} ($\times$1000) and δ_{ijkl} ($\times$10000) for the Li atom in model III.

The anharmonic correction to the Gaussian Debye–Waller factor takes the form

$$[1 - i\tfrac{4}{3}\pi^3(h^3\gamma_{111} + k^3\gamma_{222} + \cdots + hl^2\gamma_{233} + hkl\gamma_{123}) + \tfrac{2}{3}\pi^4(h^4\delta_{1111} + k^4\delta_{2222} + \cdots + k^2l^2\delta_{2233} + kl^3\delta_{2333})].$$

T (K)	γ_{111}	γ_{222}	γ_{333}	γ_{112}	γ_{122}	γ_{113}	γ_{133}	γ_{223}	γ_{233}	γ_{123}
173	0.00 (4)	0.02 (1)	−0.09 (4)	0.05 (2)	−0.01 (2)	−0.05 (2)	−0.04 (3)	−0.01 (1)	0.04 (2)	0.03 (1)
293	0.0	0.05 (2)	0.0	0.15 (4)	0.0	0.0	0.0	0.0	0.11 (3)	0.10 (3)

T (K)	δ_{1111}	δ_{2222}	δ_{3333}	δ_{1112}	δ_{1113}	δ_{1122}	δ_{1123}	δ_{1133}	δ_{1222}	δ_{1223}
173	0.00 (3)	0.09 (3)	0.04 (3)	0.03 (2)	−0.01 (2)	0.03 (1)	0.01 (1)	0.01 (2)	−0.01 (2)	0.01 (1)
293	0.01 (5)	0.20 (5)	−0.13 (4)	0.0	0.05 (4)	0.07 (3)	0.0	0.04 (3)	0.0	0.04 (2)

T (K)	δ_{1233}	δ_{1333}	δ_{2223}	δ_{2233}	δ_{2333}
173	−0.01 (1)	0.03 (2)	−0.02 (1)	0.00 (1)	−0.04 (2)
293	0.0	−0.01 (3)	0.0	0.00 (2)	0.0

'straight' pathway parallel to [001] would require the Li to overcome an additional barrier height of 435 J mol^{-1}.

Anharmonic refinement of Li in the low-temperature phase yields only an insignificant improvement over the harmonic approximation. Almost all of the 25 allowed elements of the third- and fourth-rank tensor have values within 2 s.u. (Table 3). Compared to the harmonic approximation, R is lowered from 2.85% (R_w = 6.67%) to 2.81% (R_w = 6.58%). The PDF in the (100) section is shown in Fig. 3(*b*), demonstrating the higher probability density as a result of Li ordering onto one site. The probability density at the opposite mode position of the paraphase is negligible, indicating a high degree of order (see below). Because of the problems discussed above, Li was held at $y = 0.061$. The thermal movement at T = 173 K is dominated by the direction normal to the elongation of the LiO_4 tetrahedron, a direction in which the movement of Li is least restrained and requires mainly bending of the Li—O bonds. The mean Li—O distance is 2.02 Å at 173 K and 2.05 Å at 293 K, which is similar to the mean distance observed in LTSO (Genkina & Mill, 1992) but larger than the distance of 1.95 Å calculated from effective ion radii (Shannon, 1976). The Li ordering occurs in such a way that the distance to the Ta cation along the bridge Ta—O32—Li is maximized. Thus in the ordered phase, Li is 2.08 Å apart from O31 and further from O32 (2.732 Å), as the latter O forms a short bond with Ta. A detailed picture of the displacements is given in Fig. 5.

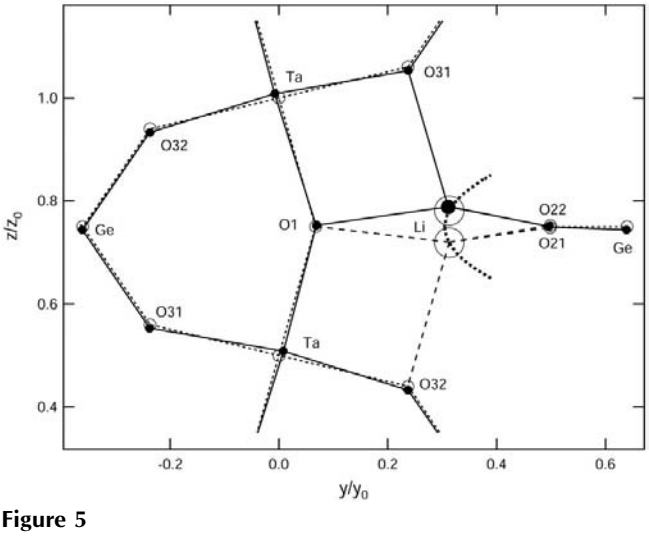

Figure 5
The structure of ordered and disordered LTGO normal to the a^* direction. The atomic positions and bonds of the paraphase are drawn as empty circles and broken lines, respectively. Filled circles and solid lines mark the atom positions in the ordered phase. The dashed curve traces the extrapolated pathway of the Li cation between the two mode positions. The O22 and O21 atoms are located 0.173a above and below the shown layer, respectively.

The atomic positions obtained in the model III refinements generally agree with those determined in the two harmonic models; thus, only the latter positions are listed in the supplementary material, except in the case of Li. The harmonic temperature coefficients of the heavier atoms Ge and Ta are about 10% smaller in the model III refinements, while the O coefficients are not separately listed as they largely agree within 1 s.u. for all refinements.

On cooling LTGO below T_c, sharp Bragg reflections appear at the $h + k = 2n + 1$ positions of reciprocal space. Hence this phase transition in LTGO corresponds to the $P2_1/c \leftrightarrow C2/c$ antiferroelectric paraelectric transition in titanite. No diffuse scattering at these positions was observable in any of the scans made at $T > T_c$. The transition is reversible and no temperature hysteresis is evident from the data.

As the transition occurs at the zone boundary of the paraphase, the squared order parameter, *i.e.* the square of the relative Ta off-centre displacement, is a linear function of the intensity at the critical-zone boundary point, $Q^2 \propto I$. This order parameter is plotted in Fig. 6, using

$$Q = sF^{1/2} = s\left(\frac{2I_{h,k,l}}{I_{h,k-1,l} + I_{h,k+1,l}}\right)^{1/2}. \quad (1)$$

Here s is a scaling factor, chosen so that $Q \rightarrow 1$ at low temperatures. The order-parameter evolution as a function of temperature is very similar to that observed in titanite. Using a mean-field model equivalent to the one used by Hayward *et al.* (2000) to describe the thermodynamic properties of the phase transition, the self-consistency equation for the equilibrium order parameter is (*cf.* Malcherek *et al.*, 1999)

$$Q = \tanh\left[\frac{T_c}{T}Q(1 + xQ^2)\right], \quad (2)$$

where $x = B/A$ is the ratio of the fourth-order coefficient, B, to the second-order coefficient, $A = -2nRT_c$, in the underlying free-energy expansion. The tricritical value, $x = \frac{1}{3}$, is valid for titanite (Hayward *et al.*, 2000) and the resulting function with $T_c = 231$ K is plotted together with the equilibrium order-parameter data in Fig. 6. Releasing the coefficient x when fitting the data gives a value slightly larger than $x = \frac{1}{3}$, which would indicate a weakly first-order phase transition, but more accurate measurements in the vicinity of T_c are needed to confirm this.

As has been suggested above, the Li atom is equally distributed over two equivalent positions, both 0.23 Å away from the diad axis in the *C*2/*c* phase. Coupled to the ordering of the Ta cations, it therefore has to condense into one of these two positions during the course of the transition to the low-temperature phase. This indicates that the transition is more of the order–disorder type than of a purely displacive nature. This is also confirmed by the applicability of the mean-field approximation (2).

4. Conclusions

The phase transition from the ordered $P2_1/c$ (antiferroelectric) to the disordered *C*2/*c* (paraelectric) structure of LTGO has been located at $T_c = 231$ (1) K. The low-temperature structure is characterized by the off-centre displacement of Ta and an ordered Li configuration. The equilibrium order parameter as a function of temperature in LTGO evolves in a manner very similar to that of titanite. Li occurs in a distorted tetrahedral oxygen coordination. For $T > T_c$, the Li atom flips back and forth between two equivalent tetrahedral positions on a curved pathway, with the common edge of the LiO_4 and GeO_4 tetrahedra as the pivot.

In LTGO, the height of the barrier between both positions is related to T_c. Thus it can be anticipated that this barrier is higher in LTSO, where the ordered phase is stable at room temperature, and that the replacement of Ge by Si has a marked effect on the stability of the ordered structure through alteration of crucial bond properties.

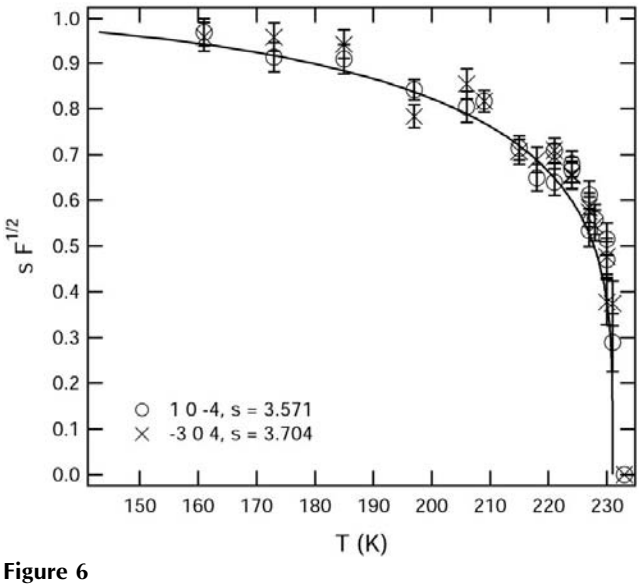

Figure 6
Temperature evolution of the order parameter, as given by the square root of the relative intensity of the reflections 104 and $\bar{3}04$. The solid curve describes the expected mean-field behaviour for a tricritical phase transition.

Financial support by *Deutsche Forschungsgemeinschaft* (MA2284) is gratefully acknowledged. The author would like to thank Sergey Matveev for carrying out the microprobe analysis.

References

Becker, P. J. & Coppens, P. (1974). *Acta Cryst.* A**30**, 129–147.
Genkina, E. A. & Mill, B. V. (1992). *Sov. Phys. Crystallogr.* **37**, 769–772.
Ghose, S., Ito, Y. & Hatch, D. M. (1991). *Phys. Chem. Miner.* **17**, 591–603.
Hayward, S. A., del Cerro, J. & Salje, E. K. H. (2000). *Am. Mineral.* **85**, 557–562.
Kek, S., Aroyo, M., Bismayer, U., Schmidt, C., Eichhorn, K. & Krane, H. (1997). *Z. Kristallogr.* **212**, 9–19.
Kuhs, W. F. (1992). *Acta Cryst.* A**48**, 80–98.
Lii, K. H., Li, C. H., Cheng, C. Y. & Wang, S. L. (1991). *J. Solid State Chem.* **95**, 352–359.
Malcherek, T., Carpenter, M. A., Kroll, H. & Salje, E. K. H. (1999). *Phys. Chem. Miner.* **26**, 354–366.
Malcherek, T., Paulmann, C., Domeneghetti, M. C. & Bismayer, U. (2001). *J. Appl. Cryst.* **34**, 108–113.
Mill, B., Belokoneva, E. & Butashin, A. (1990). *Sov. Phys. Crystallogr.* **35**, 176–180.
Shannon, R. D. (1976). *Acta Cryst.* A**32**, 751.
Sheldrick, G. M. (1997). *SHELXL*97. University of Göttingen, Germany.
Stoe & Cie (1996). *X-SHAPE* and *X-RED*. Stoe & Cie, Darmstadt, Germany.
Taylor, M. & Brown, G. (1976). *Am. Mineral.* **62**, 435–447.
Zhang, M., Salje, E. & Bismayer, U. (1997). *Am. Mineral.* **82**, 30–35.
Zucker, U. H., Perenthaler, E., Kuhs, W. F., Bachmann, R. & Schulz, H. (1983). *J. Appl. Cryst.* **16**, 358.